Received: 24 January 2023 | Revised: 11 March 2023 | Accepted: 21 March 2023

DOI: 10.1002/jccs.202300039

ARTICLE

JCCS JOURNAL OF THE CHINESE CHEMICAL SOCIETY

Corrosion resistance of amorphous $AlPO_4$ coating in salty atmospheres

Fatemehsadat Sayyedan | **Mohammadhossein Enayati** | **Masoud Taghipour** | **Pegah Ghasemizadeh**

Department of Materials Engineering, Isfahan University of Technology, Isfahan 8415683111, Iran

Correspondence
Fatemehsadat Sayyedan, Department of Materials Engineering, Isfahan University of Technology, Isfahan 8415683111, Iran.
Email: fs.sayyedan@alumni.iut.ac.ir

Abstract

The objective of the present study was to introduce a cost-effective and environmentally friendly coating to improve the corrosion resistance of the structures located in salt water. The coating solution, based on amorphous aluminum phosphate composition, was synthesized by sol–gel process and applied to AISI 304 stainless steel by dip coating technique. X-ray diffraction, scanning electron microscopy, and energy dispersive X-ray spectroscopy analyses were employed to investigate the phase composition and morphology of the coating. Corrosion behavior of the uncoated and coated samples was investigated using standard salt spray test, potentiodynamic polarization, and electrochemical impedance spectroscopy (EIS) in 3.5 wt.% NaCl solution. Salt spray test results for the bare substrate revealed a corrosion rate of six-time greater than that of the coated surface after 168 hr exposure time. Electrochemical test results declared that the amorphous $AlPO_4$ coating decreased the corrosion current density of the AISI 304 stainless steel by 10 orders of magnitude. Furthermore, according to the corresponding EIS measurements, the coated surface exhibited a superior anti-corrosion performance than uncoated sample. Overall, the results declared that the amorphous $AlPO_4$ coating could be a good choice for surface protection of stainless steel against electrochemical corrosion in salty environments.

KEYWORDS

amorphous $AlPO_4$, coating, corrosion resistance, electrochemical polarization, salt spray

1 | INTRODUCTION

Corrosion of metals and alloys in saltwater environment is a common and serious issue across many industries located in coastal areas, including the naval industry, petroleum and gas plants, and desalination plants. The combination of moisture, oxygen, and salt, especially sodium chloride, may create an aggressive environment and cause severe damage on the surface of metals, followed by weakening and falling apart of metallic structures.[1,2] In this situation, making use of more resistant materials to corrosion, such as stainless steel, is not enough, and so applying protective coatings is a reasonable solution.[3]

Corrosion mitigation in seawater would be achieved by choosing the right materials, making use of corrosion inhibitors, applying surface treatment and metal plating ornon-metallic protective coatings, regular corrosion monitoring and inspection, and cathodic protection techniques, depending on the corrosion type that occurred.[4,5] For instance, Araoyinbo et al.[6] studied the effect of sodium

nitrite as a corrosion inhibitor of mild steel in sea water. Their observations obtained from the weight loss analysis showed that 4 wt.% of sodium nitrite was able to retard the corrosion rate of mild steel. In another research, Saghi Beyragh et al.[7] evaluated corrosion resistance of hard chromium coating on mild steel substrates using direct current (DC) and pulse current (PC) electroplating processes. Although the results of the salt fog and electrochemical tests' results revealed excellent corrosion resistance in the saltwater medium for coated specimens, environmental concerns with chromate coatings and their serious drawbacks due to the high-toxicity hexavalent chromium salts, either during the surface treatment, disposal of electroplating bath, or the recycling process of coated sheets, must not be ignored.[8] Ahmad et al.[9] employed electrodeposited pure nickel and nickel–montmorillonite (Ni–MMT) nanocomposite coatings from Watts' type solution to improve the corrosion resistance of copper discs in simulated seawater. Overall, in order to cope with the side effects of environmental contamination caused by the corrosion inhibitors and common electroplating or electroless baths, employing environment-friendly sol–gel coatings could be highly efficient to combat corrosion and fouling. Many benefits, such as room temperature synthesis, chemical inertness, high corrosion resistance, and little or low health hazard, could be brought by this green synthesis method.[10]

Amorphous aluminum phosphate ($AlPO_4$) can be considered a promising anticorrosive coating material for a broad range of applications. Chemically inert nature and amorphous structure of $AlPO_4$ present excellent corrosion resistance due to the lack of crystalline defects such as grain boundaries.[11,12] The most important characteristic feature of this material is that it is environment-friendly, either in the synthesis method or the precursor used. There is no trace of use of any toxic chemicals, heavy metals, or environmental pollutants in the synthetic composition. Employing methods and precursors with no heavy metals or toxic chemicals must be an essential consideration to avoid pollution of marine resources, considering the main application of many structures in contact with salt water as a simulated seawater medium.

The objective of the present research was to introduce a cost-effective and environmentally friendly coating material to improve the corrosion resistance of offshore structures and make efficient use of marine resources efficiently. In this regard, a composition based on a synthetic aluminum phosphate, in which the molar content of aluminum is greater than phosphorus to create a pseudo-amorphous structure without use of toxic chemicals, heavy metals, or environmental pollutants, was synthesized by green sol–gel process and coated on the surface of AISI 304 stainless steel. Then, the corrosion resistance of the coated and uncoated samples was accessed by salt spray and electrochemical tests in the standard saltwater media.

2 | MATERIALS AND METHODS

A sheet of AISI 304 stainless steel with a thickness of 1 mm was cut into 20 × 20 mm^2 and ground up to 2400 grit SiC paper and then polished with 1 μm alumina slurry. The specimens were degreased in an ultrasonic bath containing acetone and deionized water for 30 min. The substrates were merged in the acid solution of HCl (37%, Sigma-Aldrich) and H_3PO_4 (85%, Sigma-Aldrich) for 1 min to create surface micro-roughness.

Non-crystalline $AlPO_4$ compound was synthesized by sol–gel process according to our previous research.[11] Aluminum nitrate nonahydrate ($Al(NO_3)_3.9H_2O$, Merck, 98.5% purity) and phosphorus pentoxide (P_2O_5, Merck, 98% purity) were dissolved in ethanol (C_2H_5OH, Merck, 99.8% purity) to reach aluminum to phosphorous ratio of 1.75:1. 5 wt. % polyvinylpyrrolidone ($(C_6H_9NO)_n$, Sigma-Aldrich) was added to the above solution and stirred for 1 hr. Stainless steel coupons were dip coated into the prepared sol for 1 min with a constant withdrawal rate of 15 mm/min. The coated samples were dried in an oven at 60°C for 12 hr and annealed in an electrical furnace at 500°C for 1 hr.

Phase composition of the coating material was analyzed by an X-ray diffractometer (XRD, Philips PW1830) using Ni-filtered Cu Kα (lCu Kα = 0.154 nm, 40 kV, 40 mA) over the 2θ range of 10°–80°. Morphology and elemental analysis of the coatings were assessed using scanning electron microscopy (SEM, Philips XL30) equipped with energy-dispersive spectroscopy (EDS), respectively. Glow discharge optical emission spectrometry (GDOES, GDA 750 HR) technique operated at 700 V and regulated pressure of 2.3 hPa was performed to achieve the composition and thickness of the coating.

The salt spray test was run according to the ASTM B117-18 standard test method for a total of 168 hr exposure time. The coated and uncoated specimens were placed in a spray chamber at an angle of 30° to vertical and continuously sprayed with 5 wt.% NaCl solution under environmental conditions of pH 7 and temperature 35°C. The weight changes of the samples were recorded after each 24 hr intervals by an electrical balance (ANDGE120) with a sensitivity of ±0.1 mg. The weight changes of the samples per unit area were plotted against the corrosion time. Three samples in each group were considered for weight change measurements, and the results were reported as an average value ± standard deviation.

Potentiodynamic polarization tests for the bare stainless steel 304 substrate and amorphous $AlPO_4$ coating were performed using the device (AMETEK model

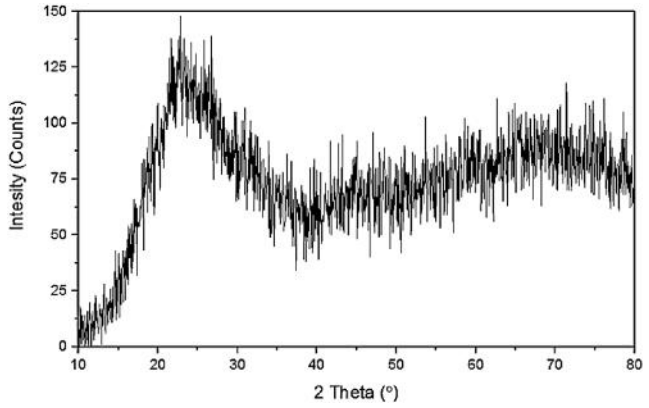

FIGURE 1 XRD pattern of the synthesized $AlPO_4$ powder after annealing at 500°C for 1 hr.

PARSTST 2237) equipped with Electrochemistry PowerSuite software in 3.5 wt.% NaCl solution at room temperature. Coated and uncoated samples with the surface area of 0.3 cm^2 were used as working electrodes. Moreover, a saturated Ag/AgCl electrode connected to a luggin capillary and a platinum sheet were employed as reference and counter electrodes, respectively. Before polarization test, specimens were kept in the electrolyte for 1 hr to reach the steady-state value of open circuit potential (OCP). The potential was then swept from −250 mV versus OCP to +300 mV versus. breakdown potential using a scan rate of 1 $mV.s^{-1}$. The electrochemical impedance spectroscopy (EIS) measurements were attained at an OCP value in the frequency range from 100 kHz to 10 mHz with an amplitude of 10 mV for the input sine-wave signal.

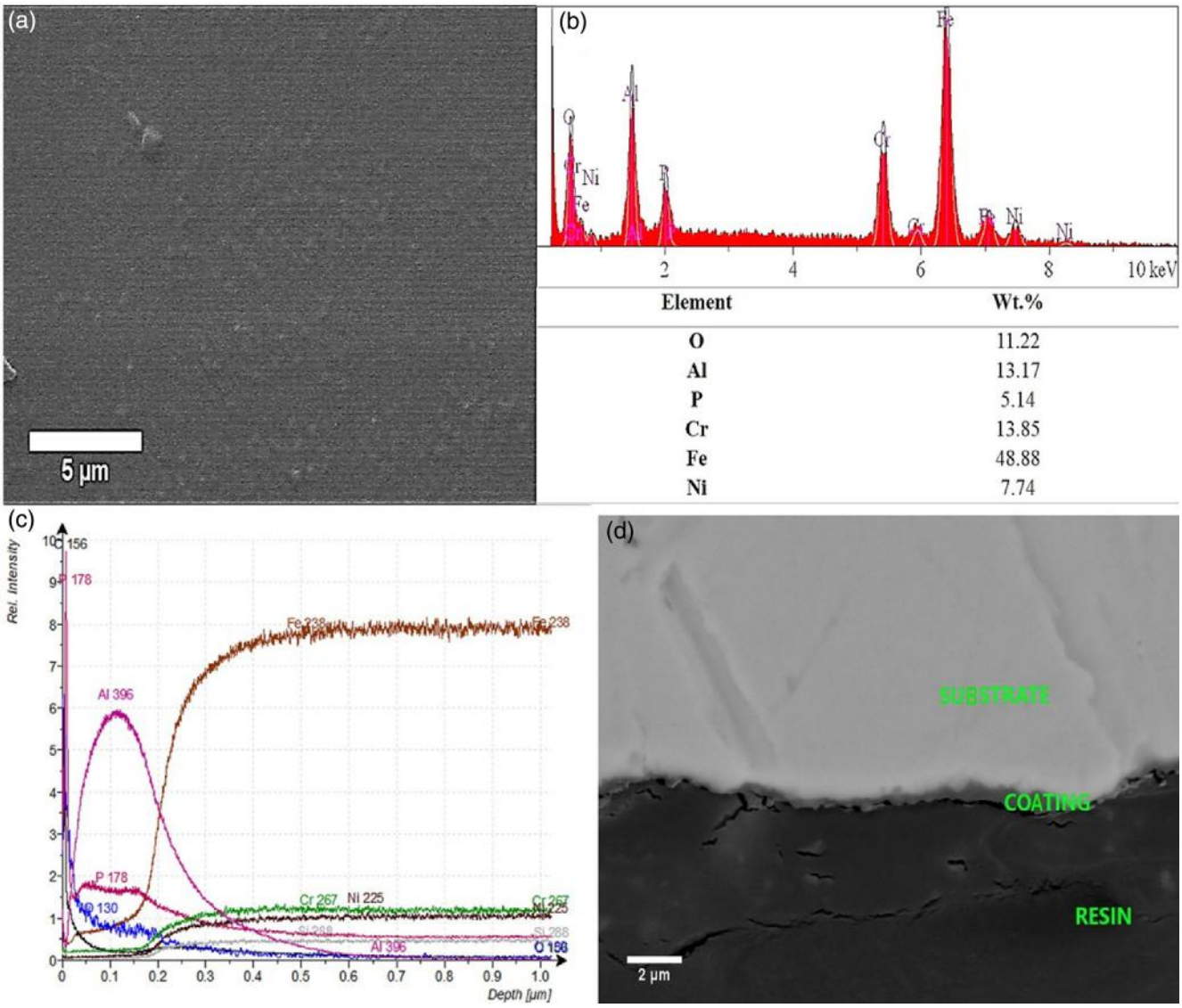

FIGURE 2 SEM, EDS, and GDOES analyses of the $AlPO_4$ coating applied on the AISI 304 stainless steel after annealing at 500°C for 1 hr: (a) surface morphology, (b) EDS analysis, (c) GDOES analysis, and (d) Cross-section morphology.

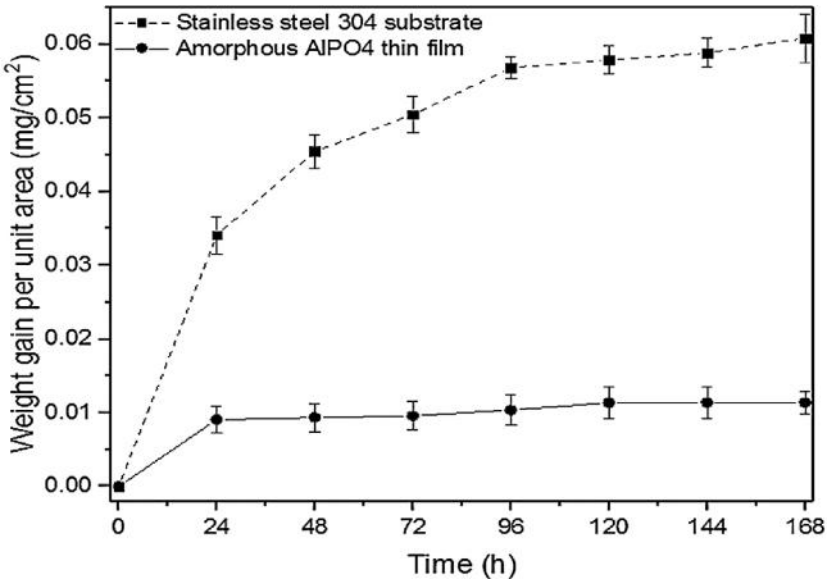

FIGURE 3 Weight changes per unit area versus corrosion time for the AISI 304 stainless steel and amorphous $AlPO_4$ coating after different exposure times in the salt spray test (error bars indicate standard deviation).

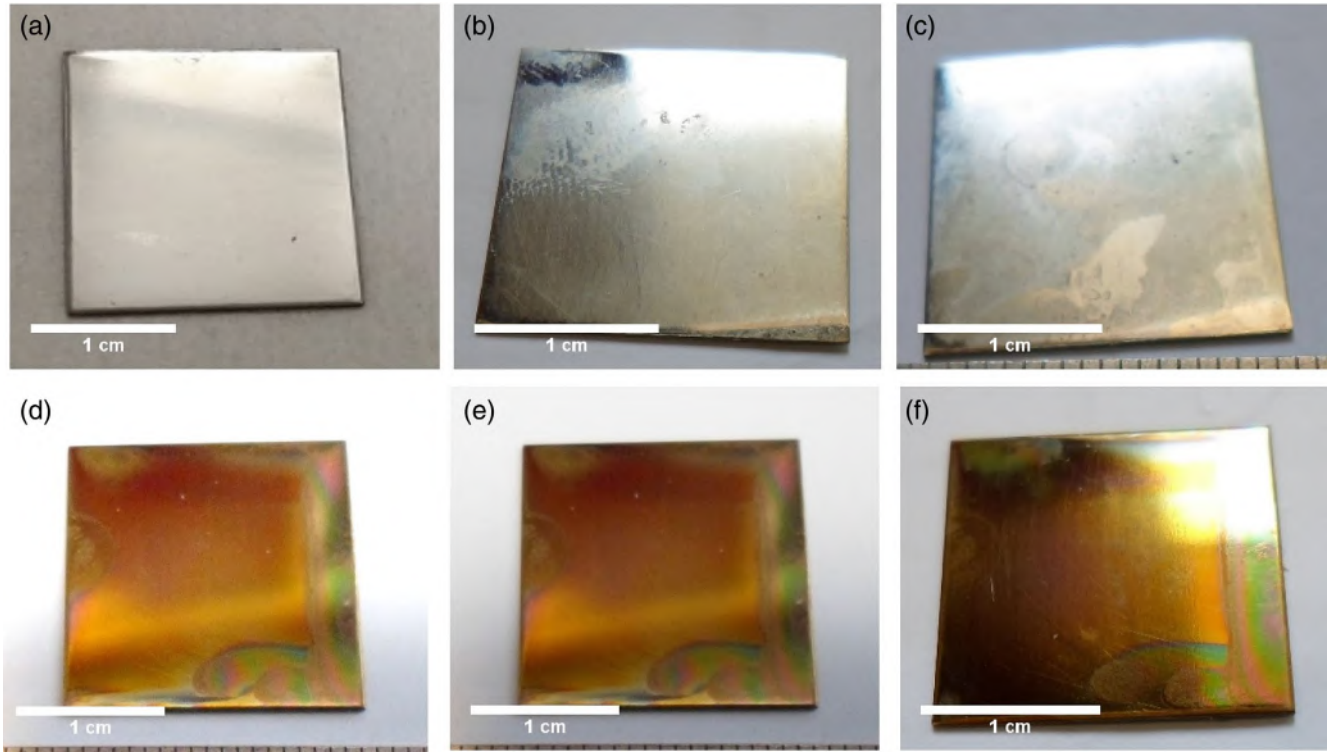

FIGURE 4 Digital photographs after specific time intervals of the salt spray test for the bare stainless steel 304 (a) before exposure, (b) after 24 hr exposure, (c) after 168 hr exposure; and amorphous $AlPO_4$-coated stainless steel (d) before exposure, (e) after 24 hr exposure, and (f) after 168 hr exposure.

3 | RESULTS AND DISCUSSION

The XRD pattern of the synthesized $AlPO_4$ powder after annealing at 500°C for 1 hr is presented in Figure 1. It could be clearly seen that the synthesized powder contains no crystalline features but a broad hump at 2θs between 20°–30°, which confirms the amorphous nature of the synthesized coating material.

Figure 2 exhibits the SEM image and EDS and GDOES analyses of the amorphous $AlPO_4$ coating applied on the surface of the stainless steel 304 after annealing at 500°C for 1 hr. As seen, the coating

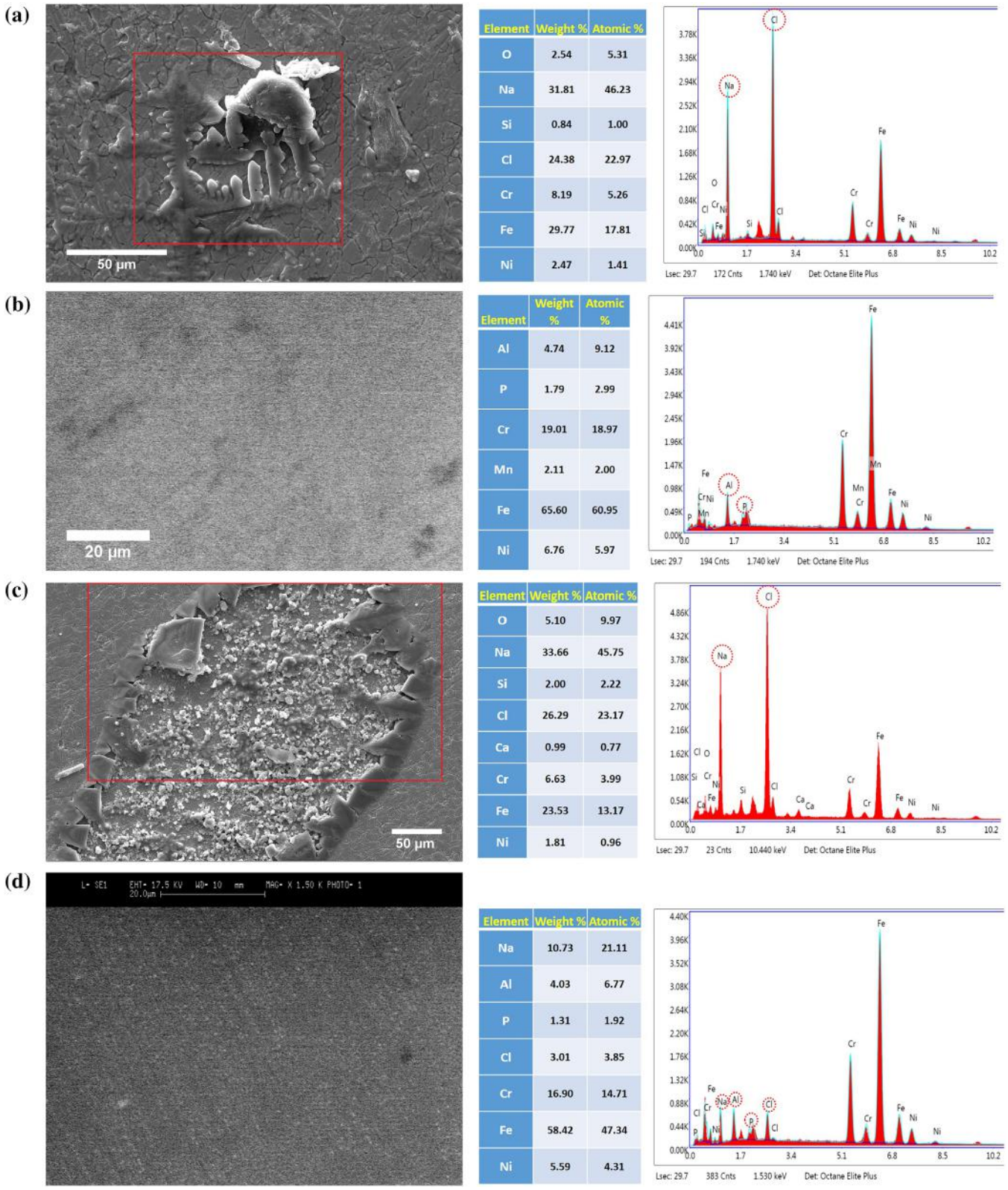

FIGURE 5 SEM images and EDS analyses of the uncoated and amorphous $AlPO_4$-coated stainless steel 304 after different exposure times in the salt fog: (a) uncoated stainless steel after 24 hr, (b) amorphous $AlPO_4$ coating after 24 hr, (c) uncoated stainless steel after 168 hr, and (d) amorphous $AlPO_4$ coating after 168 hr.

formed on the surface is uniform and continuous without any traces of microcracks (Figure 2a). EDS analysis presented in Figure 2b confirmed the formation of aluminum phosphate composition on the surface by appearing aluminum and phosphorous elements in the analysis.

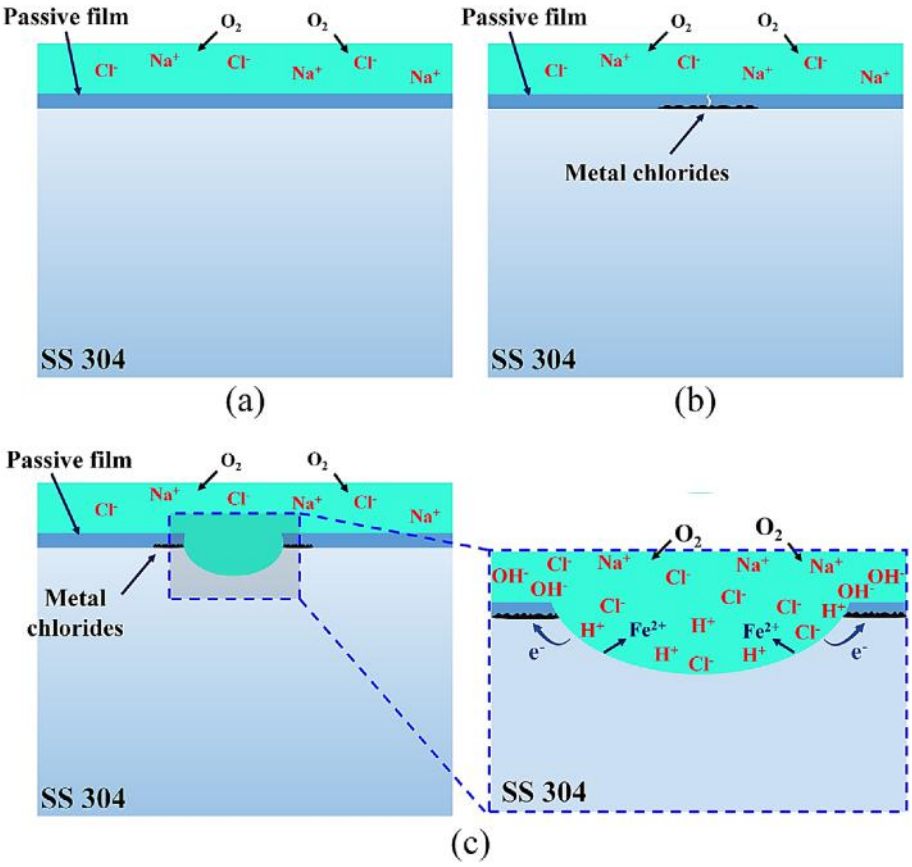

FIGURE 6 Schematic illustration of the proposed model for the formation of pits on the stainless steel 304 surface exposed to an aggressive chloride environment.

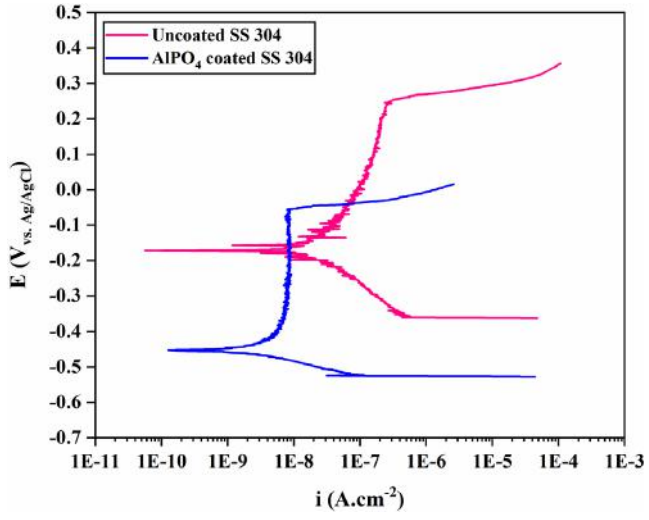

FIGURE 7 Potentiodynamic polarization curves of uncoated and $AlPO_4$-coated SS 304 in 3.5 wt.% NaCl solution.

GDOES analysis (Figure 2c) reveals, firstly, that Al and P elements have a meaningful concentration gradient in the surface region, decaying towards the depth, and secondly, that the thickness of the aluminum phosphate coating is ~300 nm, where the Fe, Cr, and Ni contents are almost constant. Figure 2d shows the cross-sectional microstructure of the thin film formed on the stainless steel substrate. It demonstrates that the coating is dense, uniform, with good adhesion to the substrate. The thickness of the thin film is estimated to be ~300 nm, which is in accordance with GDOES result.

Figure 3 represents the weight changes per unit area plotted against the corrosion time for the bare stainless steel 304 substrate and the amorphous $AlPO_4$-coated sample. There are two main points immediately evident from Figure 3:

1. The magnitude of weight gain per unit area for the bare substrate is around six times greater than that of the coated surface after 168 hr exposure time in the salt fog medium, namely 0.06 $mg.cm^{-2}$ for the bare substrate versus 0.01 $mg.cm^{-2}$ for amorphous $AlPO_4$-coated substrate.
2. Corrosion rate of the coated surface remains almost constant after 24 hr exposure time in the salt fog, while the corrosion trend of the uncoated substrate traverses ascending with time.

Digital photographs, SEM images, and EDS analyses of the uncoated and amorphous $AlPO_4$-coated stainless steel 304 after different exposure times in the salt fog are presented in Figures 4 and 5, respectively. Accordingly, corrosion products are clearly observed on the bare

TABLE 1 Electrochemical parameters obtained from potentiodynamic polarization curves of uncoated and $AlPO_4$-coated SS 304 in 3.5 wt.% NaCl solution.

Sample	E_{corr} (VSCE)	E_b (VSCE)	i_{corr} (A/cm^2)
SS 304 substrate	−0.16	0.24	1.07×10^{-8}
Amorphous $AlPO_4$ coating	−0.45	−0.05	1.18×10^{-9}

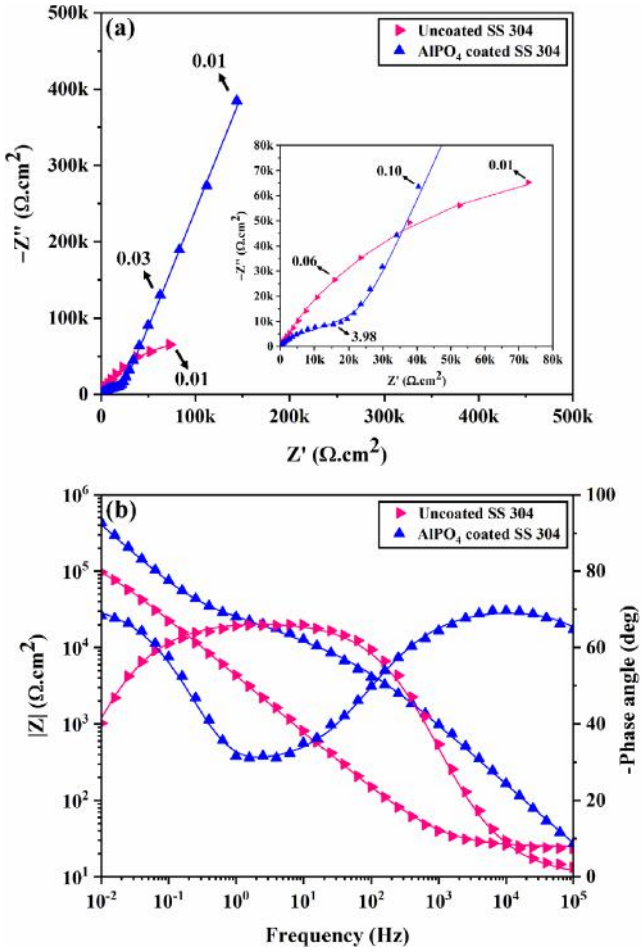

FIGURE 8 Nyquist (a) and bode (b) plots for uncoated and $AlPO_4$-coated SS 304 in 3.5 wt.% NaCl solution.

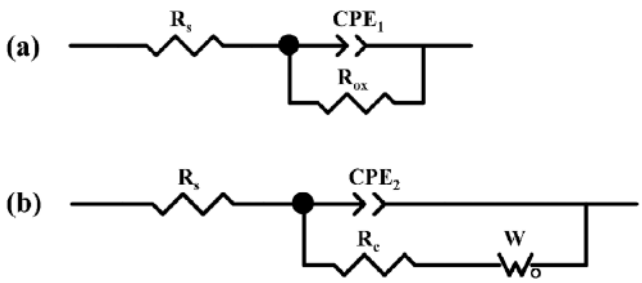

FIGURE 9 Equivalent circuits for fitting impedance spectra of (a) uncoated stainless steel 304, and (b) amorphous $AlPO_4$-coated sample.

substrate surface after 24 hr exposure (see Figures 4b and 5a). Moreover, strong peaks related to Na and Cl elements have been observed in the EDS analysis of the bare surface (Figure 5a). Reversely, there are neither symptoms of corrosion products in the SEM images nor Na and Cl peaks in the EDS analysis of the coated surface after 24 hr exposure (Figure 5b), as the digital photograph of the coated surface does not detect any obvious changes raised by the corrosion phenomenon on the surface after 24 hr exposure (compare Figure 4d,e).

Damage including some shallow pits caused by the corrosion phenomenon accompanied by strong peaks related to Na and Cl elements is immediately evident on the bare substrate surface after 168 hr exposure (Figures 4c and 5c). It is noteworthy that a passive film forms on the stainless steel surface consisting of two layers, namely the iron oxide with hydroxide outer layer and chromium oxide (Cr_2O_3) inner layer.[13] However, stainless steel 304 cannot be protected against the corrosive environment, as seen in the SEM images of the bare substrate (Figure 5a,c).

Figure 6 illustrates schematically a proposed model for the formation of pits on the stainless steel 304 surface exposed to an aggressive chloride environment. Initially, the corrosive and dense salt deposit forms on the surface of stainless steel 304 as a source of $\bar{Cl}$ ions (see Figure 6a). The $\bar{Cl}$ ions are tiny enough with high diffusivity that could pass easily through the formed passive film under the high electrical field strength in the passive films.[14] Consequently, $\bar{Cl}$ ions could react with the substrate elements at the passive film/metal interface and form metal chlorides. Since metal chloride has a much higher molar volume than metal oxide, stresses are applied to the passive film, followed by formation of some cracks across the passive film (see Figure 6b).[15] After local degradation of the passive film, the surface of the bare substrate is exposed to the corrosive environment containing NaCl, causing local dissolution of the substrate and the formation of a shallow pit (see Figure 6c). The anodic reaction that can take place inside the formed pit can be shown by the reaction below[16]:

$$Fe \leftrightarrow Fe^{2+} + 2e^{-}. \quad (1)$$

The released electrons flow to the passive surface (the cathode), where the cathodic reaction takes place[16]:

$$\tfrac{1}{2}O_2 + H_2O + 2e^{-} \leftrightarrow 2(OH^{-}). \quad (2)$$

Consumption of oxygen inside the formed shallow pit reduces the production of hydroxyl ions. On the other

TABLE 2 Fitting results of impedance spectra for corrosion of uncoated and $AlPO_4$-coated SS 304 in 3.5 wt.% NaCl solution.

Sample	R_s ($\Omega.cm^2$)	CPE_1 ($\mu F.cm^{-2}$)	CPE_2 ($\mu F.cm^{-2}$)	R_{ox} ($\Omega.cm^2$)	R_c ($\Omega.cm^2$)	W ($\Omega.cm^2$)
SS 304 substrate	23.87	5.78E-5	-	201,750	-	-
Amorphous $AlPO_4$ coating	24.65	-	2.27E-07	-	23,659	190,270

hand, accumulation of Fe^{2+} ions leads to the adsorption of negatively charged chloride ions, followed by the formation of ferrous chloride in the pit. Furthermore, ferrous chloride can be hydrolyzed to produce ferrous hydroxide along with chloride ions and hydrogen. These ions intensify the corrosion at the bottom of the pit.[16,17]

On the other hand, very scarce symptoms of corrosion products, accompanied by weak Na and Cl peaks compared with the uncoated substrate, could be observed on the amorphous $AlPO_4$-coated substrate after 168 hr exposure (Figures 4f and 5d). The protective effect of the amorphous $AlPO_4$ coating against corrosion phenomena could be directly refer to the chemically inert nature and amorphous structure of the coating material.[12]

Figure 7 shows the potentiodynamic polarization curves (Tafel plots) for the bare stainless steel 304 substrate and amorphous $AlPO_4$-coated surface in 3.5 wt.% NaCl solution. The values of corrosion potential (E_{corr}) and corrosion current density (i_{corr}) extracted from Tafel polarization curves are summarized in Table 1. Accordingly, the corrosion current density for the amorphous $AlPO_4$-coated substrate has been reduced compared to the bare substrate. Values of the corrosion current density for the amorphous $AlPO_4$ coating and the bare substrate were obtained to be 1.18×10^{-9} A/cm^2 and 1.07×10^{-8} A/cm^2, respectively. This shows that the amorphous $AlPO_4$ coating has behaved as a protective layer and protected the substrate against the aggressive chloride ions.[18,19] On the other hand, the slight slope of the anodic curve of the bare substrate indicates a quasi-passive behavior. Reversely, the anodic curve of the amorphous $AlPO_4$ coating presents passive behavior, which could be attributed to its amorphous structure. Due to the lack of corrosion-prone areas, the amorphous structure prevents the local corrosion and forms a more stable passive film on the surface with the least defects compared to the bare substrate.[20]

Using the electrochemical impedance method, the Nyquist and Bode diagrams of the bare 304 stainless steel substrate and the amorphous $AlPO_4$-coated surface were investigated (Figure 8). It is well known that a larger loop in the Nyquist model indicates greater corrosion resistance.[21] The Nyquist plot obtained for the bare substrate contains a capacitive semicircular representing the oxide capacitance. For the coated sample, the first time constant at high frequencies represents the coating resistance (from 100 kHz to 3.98 Hz), and the second time constant at low frequencies (from 3.98 to 0.01 Hz) illustrates the transmission phenomena through the pores of the film (Warburg impedance). In other words, the arc of the capacitive semicircle progressively transforms into a straight line at low frequencies, exhibiting the characteristics of Warburg impedance and indicating the corrosion process is controlled by diffusion.[18] Figure 9a shows the most appropriate electrical model to explain the corrosion process of the bare sample. In this model, R_s is the solution resistance between specimens and reference electrode, and R_{ox} and CPE_1 are the resistance and constant phase elements of the passive film, respectively. On the other hand, the equivalent circuit shown in Figure 9b was used to model the electrochemical behavior of the coated sample. In this case, R_s is solution resistance, Z_w represents Warburg impedance, and R_c and CPE_2 show the resistance and constant phase elements of coating, respectively. Corresponding values extracted from the Nyquist plots are given in Table 2.

For the bare 304 stainless steel, a passive oxide layer develops as a protective layer when the substrate is exposed to the electrolyte. Therefore, the decent corrosion performance of the bare sample can be attributed to the formation of the passive oxide layer.[22] Furthermore, the Bode-phase diagram of the bare sample (Figure 8b) shows a stable zone for a broad frequency range, verifying the existence of the passive layer. For the $AlPO_4$-coated sample, in addition to the coating resistance, there is a Warburg resistance due to the diffusion of electrolyte through the coating porosities. The sum of these two resistances exceeds the resistance of the passive layer for the bare substrate, probably suggesting the superior corrosion performance of the coated sample. Additionally, according to the Bode-phase diagram of the coated sample shown in Figure 8b, the first peak at high frequencies is related to ion transfer resistance. Therefore, the corrosion performance of the coated sample has improved under ion transfer resistance at high frequencies.

It is worth noting that the absolute value of impedance at low frequencies is considered a measure of a coating's ability to prevent corrosion. As a general rule, the larger $|Z|$ at low frequencies, the better corrosion resistance.[19] According to Figure 8b, the amount of $|Z|$ at low frequencies is higher for the amorphous $AlPO_4$-

coated sample than the bare substrate. In general, the results of the EIS test were in agreement with the results of the potentiodynamic polarization test.

4 | CONCLUSIONS

The AISI 304 stainless steel alloy was dip coated in amorphous $AlPO_4$ sol, and corrosion behavior of the coated and uncoated specimens was evaluated by a standard salt spray test and electrochemical measurements. The main results were obtained as follows:

1. Salt spray test results of the bare substrate revealed a corrosion rate six times greater than that of the coated surface after 168 hr exposure time.
2. Electrochemical test results showed that the amorphous $AlPO_4$ coating decreased the corrosion current density of the AISI 304 stainless steel by 10 orders of magnitude.
3. The EIS data showed the presence of a single time constant for the bare substrate, while the amorphous $AlPO_4$ coating revealed a two-time constant, indicating improved corrosion resistance for the coated sample.
4. Overall, the results showed that the amorphous $AlPO_4$ coating was well capable of surface protection of stainless steel against corrosion in salty environments.

ACKNOWLEDGMENTS

The authors would like to express their sincere gratitude to Dr. Abdoulmajid Eslami from the Department of Materials Engineering, Isfahan University of Technology, and Tara Coatings Company, Isfahan, Iran, for the providing required equipment in this research.

ORCID

Fatemehsadat Sayyedan https://orcid.org/0000-0003-1880-3031

REFERENCES

[1] J. B. Memet, in *Corrosion of metallic heritage artefacts* (Eds: P. Dillmann, G. Béranger, P. Piccardo, H. Matthiesen), Woodhead Publishing, Sawston, **2007**, p. Chapter 9.
[2] B. Valdez, J. Ramirez, A. Eliezer, M. Schorr, R. Ramos, R. Salinas, *J. Marine Eng. Technol.* **2016**, *15*, 124.
[3] A. Garcia, B. Valdez, M. Schorr, R. Zlatev, A. Eliezer, J. Hadad, *J. Marine Eng. Technol.* **2010**, *9*, 3.
[4] X. Hou, L. Gao, Z. Cui, J. Yin, *IOP Conf. Series Earth Environ. Sci.* **2018**, *108*, 022037.
[5] M. A. El-Reedy, in *Offshore structures* (Ed: M. A. El-Reedy), Gulf Professional Publishing, Boston **2012**. Chapter 6.
[6] A. O. Araoyinbo, M. A. A. Mohd Salleh, M. Z. Jusof, *IOP Conf. Series Mater. Sci. Eng.* **2018**, *343*, 012012.
[7] M. R. Saghi Beyragh, A. S. Khameneh, S. Norouzi, *Surf. Coat. Technol.* Wiley, Hoboken, **2010**, 205, 2605.
[8] O. Gharbi, S. Thomas, C. Smith, N. Birbilis, *npj Mater. Degrad.* **2018**, *2*, 12.
[9] Y. H. Ahmad, J. Tientong, N. D'Souza, T. D. Golden, A. M. A. Mohamed, *Surf. Coat. Technol.* **2014**, *242*, 170.
[10] R. Ciriminna, M. Pagliaro, G. Palmisano, *The sol-gel handbook*, Wiley, Hoboken, **2015**. Chapter 8.
[11] F. S. Sayyedan, M. H. Enayati, M. Hashempour, A. Vicenzo, M. Bestetti, *Surf. Coat. Technol.* **2018**, *351*, 128.
[12] Z. Q. Hu, A. M. Wang, H. F. Zhang, in *Modern inorganic synthetic chemistry*, Second ed. (Eds: R. Xu, Y. Xu), Elsevier, Amsterdam **2017**, p. Chapter 22.
[13] C. C. A. D. M. Morales, *Int. J. Electrochem. Sci.* **2016**, *11*, 8683.
[14] S. Deng, S. Wang, L. Wang, J. Liu, Y. Wang, *Int. J. Electrochem. Sci.* **2017**, *12*, 1106.
[15] S. A. Saadi, Y. Yi, P. Cho, C. Jang, P. Beeley, *Corros. Sci.* **2016**, *111*, 720.
[16] R. T. Loto. Pitting corrosion evaluation of austenitic stainless steel type 304 in acid chloride media, 2013.
[17] T. Charng, F. Lansing. Review of corrosion causes and corrosion control in a technical facility, in, United States, 1982, Chapter 1.
[18] Z. Ding, Y.-Y. Li, M.-R. Xu, X. Hong, S.-X. Hong, B. Dong, *Construc. Build. Mater.* **2020**, *251*, 118874.
[19] X. Huang, D. Wang, Y. Dong, *Surf. Coat. Technol.* **2020**, *382*, 125242.
[20] G. S. Frankel, J. D. Vienna, J. Lian, J. R. Scully, S. Gin, J. V. Ryan, J. Wang, S. H. Kim, W. Windl, J. Du, *npj Mater. Degrad.* **2018**, *2*, 15.
[21] H. Luo, Z. Li, A. M. Mingers, D. Raabe, *Corros. Sci.* **2018**, *134*, 131.
[22] S. V. Phadnis, A. K. Satpati, K. P. Muthe, J. C. Vyas, R. I. Sundaresan, *Corros. Sci.* **2003**, *45*, 2467.

How to cite this article: F. Sayyedan, M. Enayati, M. Taghipour, P. Ghasemizadeh, *J. Chin. Chem. Soc.* **2023**, 1. https://doi.org/10.1002/jccs.202300039